Localization of Cys^{133} of Rabbit Skeletal Troponin-I with Respect to Troponin-C by Resonance Energy Transfer

Yin Luo,* Jing-Lun Wu,* John Gergely,*#§ and Terence Tao*¶‖

*Muscle Research Group, Boston Biomedical Research Institute, Boston, Massachusetts 02114; #Neurology Service, Massachusetts General Hospital, Boston, Massachusetts 02114; §Department of Biological Chemistry and Molecular Pharmacology and ¶Department of Neurology, Harvard Medical School, Boston, Massachusetts 02115; and ‖Department of Biochemistry, Tufts University School of Medicine, Boston, Massachusetts 02111 USA

ABSTRACT We have used the technique of resonance energy transfer in conjunction with distance geometry analysis to localize Cys^{133} of troponin-I (TnI) with respect to troponin-C (TnC) in the ternary troponin complex and the binary TnC·TnI complex in the presence and absence of Ca^{2+}. Cys^{133} of TnI was chosen because our previous work has shown that the region of TnI containing this residue undergoes Ca^{2+}-dependent movements between actin and TnC, and may play an important role in the regulatory function of troponin. For this purpose, a TnI mutant with a single Cys at position 133, and TnC mutants, each with a single Cys at positions 5, 12, 21, 41, 49, 89, 98, 133, and 158, were constructed by site-directed mutagenesis. The distances between TnI Cys^{133} and each of the nine residues in TnC were then measured. Using a least-squares minimization procedure, we determined the position of TnI Cys^{133} in the coordinate system of the crystal structure of TnC. Our results show that in the presence of Ca^{2+}, TnI Cys^{133} is located near residue 12 beneath the N-terminal lobe of TnC, and moves away by 12.6 Å upon the removal of Ca^{2+}. TnI Cys^{133} and the region of TnC that undergoes major change in conformation in response to Ca^{2+} are located roughly on opposite sides of TnC's central helix. This suggests that the region in TnI that undergoes Ca^{2+}-dependent interaction with TnC is distinct from that interacting with actin.

INTRODUCTION

Mammalian striated muscle is regulated by the interaction of Ca^{2+} with the regulatory protein troponin (Tn), which, in concert with tropomyosin, modulates the cyclic interaction between myosin heads and actin. Tn is composed of the Ca^{2+}-binding, inhibitory, and tropomyosin-binding subunits (TnC, TnI, and TnT, respectively). The crystal structure of TnC reveals a dumbbell-shaped molecule with its N- and C-terminal domains well separated by a single central α-helix (Herzberg and James, 1985; Sundaralingam et al., 1985). The C-domain contains two high-affinity Ca^{2+}-binding sites that bind Mg^{2+} as well, but with ~1000-fold lower affinity. The N-domain contains the two low-affinity, physiologically relevant, Ca^{2+}-binding sites. Binding of Ca^{2+} to these sites causes the joint movement of the B-helix and C-helix, whereupon a hydrophobic patch becomes exposed (Fujimori et al., 1990; Grabarek et al., 1990; Herzberg et al., 1986; Slupsky and Sykes, 1995; Wang et al., 1992), available for interaction with some portion of TnI, triggering further events in the regulatory process (for reviews, see Farah and Reinach, 1995; Grabarek et al., 1992). The detailed mechanism of these processes is not well understood, primarily because little is known about the structure of the Tn complex. A study using fragments of TnI and TnC suggested that the two proteins interact with each other in an antiparallel manner (Farah et al., 1994). Our own photo-cross-linking results are consistent with such an arrangement (Kobayashi et al., 1994). A low-angle neutron and x-ray scattering study produced a structural model in which TnI wraps around the central helix of TnC and forms two "cap" regions above and below the N- and C-domains of TnC (Olah et al., 1994; Olah and Trewhella, 1994).

Ideally, high-resolution structural information derived from x-ray crystallography or heteronuclear NMR is desirable to fully understand the structures of protein complexes and the mechanisms of protein functions. When such high-resolution structures were unavailable, the technique of resonance energy transfer (RET) (Fairclough and Cantor, 1978; Stryer, 1978) was used to obtain structural information. Before the availability of crystal structures of actin and myosin subfragment 1, for example, distances derived from RET measurements were used to deduce the spatial arrangements of certain residues in these proteins (e.g., Botts et al., 1989; Kekic et al., 1996; Miki et al., 1992, and references therein; Park et al., 1991). Although a complex of an N-terminal fragment of TnI and TnC has recently been crystallized (Saijo et al., 1997), no crystal of Tn or of a complex containing intact TnI has been available for x-ray diffraction. We (Tao et al., 1989) and others (Wang and Cheung, 1986) have used RET to measure distances between various sites in these complexes. In these early studies, only a few distances could be measured, because the Tn complex has only four indigenous Cys residues to which donor-acceptor probes could be attached. With the advent of site-directed mutagenesis, it has become possible to construct TnC and TnI mutants that contain cysteines at defined sites. Thus several distances could be measured both within and between the subunits (e.g., Dong et al., 1997; Gong et al., 1994; Luo et al., 1997; Wang et al., 1992).

Received for publication 29 September 1997 and in final form 17 February 1998.

Address reprint requests to Dr. Terence Tao, Boston Biomedical Research Institute, 20 Staniford Street, Boston, MA 02114. Tel.: 617-742-2010; Fax: 617-523-6649; E-mail: tao@bbri.harvard.edu.

0006-3495/98/06/3111/09 $2.00

In this work, we constructed a rabbit skeletal TnI mutant with a single cysteine at position 133 (I133) and nine TnC mutants, each with a single cysteine at positions 5, 12, 21, 41, 49, 89, 98, 133, and 158 (C5, C12, etc.), and applied RET in conjunction with distance geometry analysis to locate Cys^{133} of TnI in relation to the nine positions in TnC. Cys^{133} of TnI was chosen because we have shown that the region containing this residue undergoes reversible Ca^{2+}-dependent movements between actin and TnC (Tao et al., 1989, 1990) and has been suggested to play an important role in the regulation process (Kobayashi et al., 1994; Pearlstone et al., 1997). Using *N*-iodoacetyl-*N*′-(5-sulfo-1-naphthyl)ethylenediamine (1,5-IAEDANS) as the fluorescent donor and either 4-dimethylaminophenylazophenyl-4′-maleimide (DAB-Mal) or *N*-(4-dimethylamino-3,5-dinitrophenyl)maleimide (DDP-Mal) as the nonfluorescent acceptor, the distances between Cys^{133} of TnI and the cysteine residues in each TnC mutant were measured by RET. The position of TnI residue 133 was then determined in the framework of the crystal structure of TnC by least-squares minimization of the differences between the measured distances and those calculated using coordinates derived from the crystal structures of TnC. The results have significant implications for the conformation of TnI in the Tn complex and for the mechanism of Tn function.

EXPERIMENTAL PROCEDURES

Chemicals

Common reagents were from Sigma. HEPES was from Research Organics (Cleveland, OH). 1,5-IAEDANS was from Aldrich (Milwaukee, WI), and DDP-Mal and DAB-Mal were from Molecular Probes (Eugene, OR). Materials for recombinant DNA procedures were from Life Technologies, and materials for gel electrophoresis were from Bio-Rad (Beverly, MA).

Myofibrils and protein preparations

Myofibrils were prepared from rabbit skeletal muscle, and their endogenous TnC and TnI were extracted as described previously (Luo et al., 1997, and references therein). TnC, TnI, and TnT were purified from rabbit skeletal muscle according to established methods (Greaser and Gergely, 1973). Single cysteine mutants of TnC were also prepared by procedures described by Wang et al. (1990). I133 cDNA was constructed by converting the TGC codons for Cys^{48} and Cys^{64} to the TCC codon for serine. The expression and purification procedures were described previously (Luo et al., 1997).

Labeling of TnC mutants with either 1,5-IAEDANS or DAB-Mal or DDP-Mal was performed in a medium containing 10 mM HEPES (pH 7.5), 0.1 M NaCl, and 2 mM EDTA. I133 was labeled in a denaturing solution containing 10 mM HEPES (pH 7.5), 4 M guanidinium chloride, 2 mM EDTA, and 0.1 M NaCl. The TnC or TnI solutions, typically 40 μM, were incubated with 5–10 mM dithiothreitol (DTT) for 30 min and dialyzed against the above buffer solutions, but without DTT. This was immediately followed by incubation with the label (120–150 μM) for 3 h at room temperature and then overnight at 4°C. The reactions were quenched with 10 mM DTT, and excess reagents were removed by dialysis. The labeling ratios were determined spectroscopically, using extinction coefficients as in previous works (Luo et al., 1997; Wang et al., 1992). Typical molar labeling ratios were ~0.5 (label:protein) for the dansyl moiety of 1,5-IAEDANS (DAN) and >0.8 for the dimethylaminophenylazophenyl moiety of DAB-Mal (DAB) or the dimethylamino-dinitrophenyl moiety of DDP-Mal (DDP). Upon reconstitution of the binary and ternary complexes, the desired protein components were mixed stoichiometrically in the denaturing solution described above, then dialyzed against buffer solution containing 10 mM HEPES (pH 7.5), 0.1 M NaCl, and 0.2 mM $CaCl_2$.

ATPase activities of myofibrils

The regulatory activities of I133 before and after chemical modification were assessed by the ATPase activities of the extracted myofibrils reconstituted with skeletal TnC and mutant TnI's, following a procedure from our previous work (Luo et al., 1997).

Fluorescence measurements and data analysis

Fluorescence and anisotropy decay curves were obtained using a modified ORTEC9200 nanosecond fluorometer as described previously (Tao and Cho, 1979). Fluorescence decay curves were analyzed by the method-of-moments (MOM), using the program FLUOR (Small and Isenberg, 1976) to obtain τ_d and τ_{da}, the donor fluorescence lifetime in the absence and presence of acceptor, respectively. According to Förster's equations (Fairclough and Cantor, 1978), energy transfer efficiency and distance can be calculated as

$$E = 1 - \tau_{da}/\tau_d \tag{1}$$

$$R = R_o(E^{-1} - 1)^{1/6} \tag{2}$$

where R_o is the critical transfer distance corrected for the variation in donor fluorescence quantum yield, using the equation

$$R_o = R'_o(\tau_d/\tau'_d)^{1/6} \tag{3}$$

with R'_o = 39.9 Å and τ'_d = 13.5 ns, as measured previously for the DAN-DAB couple (Tao et al., 1983), and R'_o = 29 Å and τ'_d = 20.6 ns for the DAN-DDP couple (Dalbey et al., 1983).

To determine the position of TnI residue 133, we used a nonlinear least-squares fitting program, which first computes the calculated distance between the TnI and TnC residues:

$$R_{ic} = \sqrt{(x_i - X)^2 + (y_i - Y)^2 + (z_i - Z)^2} \tag{4}$$

where x_i, y_i, and z_i are the coordinates of the ith TnC residue's α-carbon in the coordinate system of the TnC crystal structure (Herzberg and James, 1985), and X, Y, and Z are those of Cys^{133} of TnI. It then computes the mean squared residual:

$$r^2/N = \frac{1}{N}\sum_{i=1}^{N}(R_i - R_{ic})^2 \tag{5}$$

where R_i are the experimental RET-determined distances, and N is the number of distances measured. r^2/N is then minimized using X, Y, and Z as variable parameters.

RESULTS

Regulatory activities

The regulatory activities of all of the TnC mutants used in this work were tested using TnC extracted myofibrils and were found to be intact (Tao et al., 1995; details will be published elsewhere). The activities of unmodified and modified I133 were examined in this work using rabbit skeletal myofibrils from which the indigenous TnC and TnI had been extracted. The ATPase activity of the extracted

myofibrils was ~100 nmol of P_i/(mg·min) and was Ca^{2+}-insensitive. The addition of unmodified I133 alone reduced the ATPase activity ~10-fold in a Ca^{2+}-insensitive manner (Table 1). When unlabeled I133 or $I133^{DAN}$ (DAN-labeled I133) was added to the myofibrils, together with rabbit skeletal TnC, the myofibrilar ATPase activity was increased by Ca^{2+} to a value close to that obtained when rabbit skeletal TnI was added with TnC. These results indicate that neither the Cys→Ser mutations at positions 48 and 64 nor the chemical modification at position 133 affected the biological activities of TnI.

Analysis of fluorescence decay curves and distance calculations

We found that the RET decay data for the complexes of I133 with the TnC mutants (with or without TnT) fall into two groups, depending on the distance, R, between the two probes. For group 1, which comprises complexes containing C41, C49, C133, and C158, R is comparable to or greater than the critical transfer distance, R_o, of the DAN-DAB couple, viz., ~40 Å. For group 2, which comprises complexes containing C5, C12, C21, C89, and C98, R is comparable to or less than R_o of the DAN-DDP couple, viz., ~30 Å.

As an example of group 1, we describe the data set for the ternary complex containing C41 in detail to illustrate our data analysis procedure. The fluorescence decay of $C41^{DAN} \cdot I133 \cdot T$ in the Ca^{2+} state (all four metal-binding sites occupied by Ca^{2+}, simulating the in vivo activated state) appears to be monoexponential (Fig. 1 *A*, *upper curve*); MOM analysis yielded a lifetime of 15.15 ns (Table 2). Biexponential MOM analysis yielded a second decay component of negligible amplitude without significantly affecting the lifetime of the major component or the value of χ^2/N (Table 2), the quality of fit parameter. We conclude that the donor decay in the absence of acceptor is monoexponential, and that the lifetime can be taken as the unquenched lifetime, τ_d, in Eqs. 1 and 2 for the distance calculations.

TABLE 1 Regulatory activities of I133 and $I133^{DAN}$

Materials	ATPase activities (nmol P_i/mg-min)	
	$+Ca^{2+}$	$-Ca^{2+}$
Myofibril(ΔIC)	100	100
Myofibril(ΔIC) + I133	9	8
Myofibril(ΔIC) + I + C	143	21
Myofibril(ΔIC) + I133 + C	136	25
Myofibril(ΔIC) + $I133^{DAN}$ + C	135	21

Myofibril (ΔIC): rabbit skeletal myofibrils with indigenous TnC and TnI extracted. Solution conditions for the $+Ca^{2+}$ state: 60 mM KCl, 30 mM imidazole, pH 7.0, 2 mM $MgCl_2$, 5 mM DTT, 2 mM ATP, 0.2 mM $CaCl_2$; for the $-Ca^{2+}$ state, 2 mM EGTA and 6 mM additional $MgCl_2$ were added. All experiments were done at 22°C.

The decay of $C41^{DAN} \cdot I133^{DAB} \cdot T$ is clearly not monoexponential (Fig. 1 *A*, *lower curve*). Whereas biexponential analysis yielded two components with comparable amplitudes, triexponential analysis yielded a third component of negligible amplitude without appreciably affecting the lifetimes of the other two components or the value of χ^2/N (Table 2). Hence we conclude that the decay of $C41^{DAN} \cdot I133^{DAB} \cdot T$ is essentially biexponential, with a short lifetime of 7.41 ns and a long lifetime of 16.99 ns (Table 2). The long lifetime is similar to the unquenched lifetime of 15.15 ns, and is attributable to those donors that are not paired with acceptors (owing, e.g., to incomplete acceptor labeling of I133). The short lifetime clearly corresponds to donors undergoing energy transfer to the acceptors, and can be taken as τ_{da}, the quenched lifetime, in Eq. 1. With $\tau_d = 15.15$ ns and $\tau_{da} = 7.41$ ns, Eqs. 1 and 2 yielded $E = 0.510$, and $R = 40.4$ Å for the Förster distance between probes attached at residues 41 of TnC and 133 of TnI. When this distance was measured with the DAN donor on I133 and the DAB acceptor on C41, we obtained 37.2 Å, which is similar to the value measured with the donor on TnI.

Fig. 1 *B* shows fluorescence decays of the same samples in the Ca^{2+}-free state (with only the high-affinity sites in TnC occupied by Mg^{2+}, simulating the in vivo relaxed state). The extent of donor quenching by the acceptor is noticeably less in this state than in the Ca^{2+} state, indicating a decrease in the extent of energy transfer and an increase in the donor-acceptor separation distance. For quantitave analysis, we again took the lifetime derived from monoexponential analysis of the $C41^{DAN} \cdot I133 \cdot T$ decay (14.76 ns; Table 2) as τ_d, and the short lifetime derived from the biexponential analysis of the $C41^{DAN} \cdot I133^{DAB} \cdot T$ decay (11.94 ns) as τ_{da}, yielding $E = 0.205$, and $R = 49.5$ Å, a distance that is 9 Å larger than that for the Ca^{2+} state.

To assess whether the measured distances are acceptor-dependent, we also measured this distance using DDP as the acceptor. Applying the same criteria as above, we found the decay of $C41^{DAN} \cdot I133^{DDP} \cdot T$ to be essentially monoexponential, with a lifetime of 13.34 ns (Table 2). Taking this as τ_{da} and 15.15 ns as τ_d, we obtained $E = 0.119$ and $R = 38.4$ Å, a distance that agrees reasonably well with that obtained using DAB as the acceptor (40.4 Å). We noted, however, that because R_o for the DAN-DDP couple (~30 Å) is considerably smaller than the distance involved (~40 Å), the transfer efficiency was very low, and MOM analysis could not distinguish the quenched lifetime from the unquenched one. When this is the case, the measurement is no longer sensitive to the increase in distance, as exemplified by the results of $C41^{DAN} \cdot I133^{DDP} \cdot T$ in the Ca^{2+} state (37.2 Å) and the Ca^{2+}-free state (37.8 Å) (Table 2). Thus it is clear that for this complex, the distance determined using DAB as the acceptor is more reliable than that using DDP, and was used in subsequent distance geometry calculations.

Because the characteristics of the data for the other members of this group were similar, they were treated in the same manner. The resultant distances are shown in Table 3

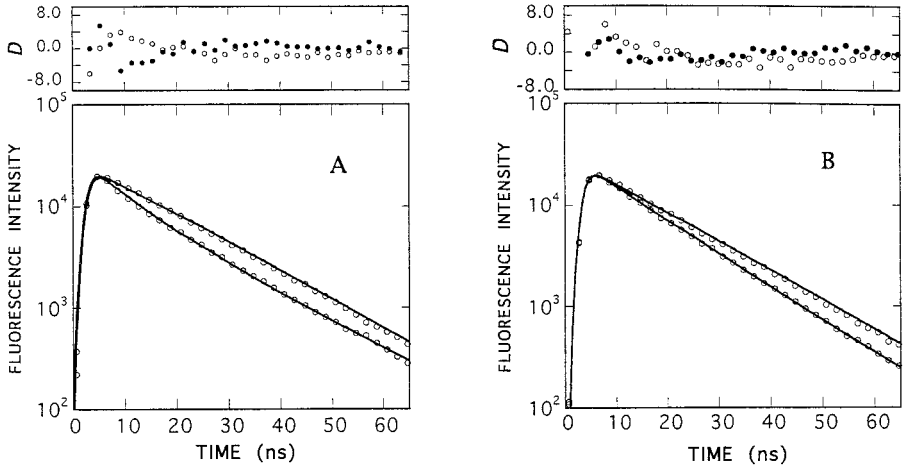

FIGURE 1 Fluorescence decay curves of $C41^{DAN} \cdot I133 \cdot T$ (*upper curves*) and $C41^{DAN} \cdot I133^{DAB} \cdot T$ (*lower curves*) in the presence (*A*) and absence (*B*) of Ca^{2+}. Circles are experimental points, shown one for every three; solid lines are calculated curves, using parameters derived from MOM analyses (Table 2). *Upper panel*: The deviation function for the upper and lower curves (*open and filled circles*, respectively). The deviation function is defined as $D_i = (I_{ie} - I_{ic})/I_{ie}^{1/2}$, where I_{ie} and I_{ic} are experimental and calculated fluorescence intensities, respectively.

(all of the fluorescence decay analysis results are available upon request).

For complexes in the second group, we have chosen the data for $C5 \cdot I133 \cdot T$ as an example. The decay of $C5^{DAN} \cdot I133 \cdot T$ is monoexponential, as expected for donor alone samples (Table 2), and the lifetime (16.78 ns) can be taken as τ_d. The decay of $C5^{DAN} \cdot I133^{DDP} \cdot T$ is biexponential and is readily interpretable as containing a quenched and an unquenched component, as described above for $C41^{DAN} \cdot I133^{DAB} \cdot T$. Taking the lifetime of the quenched component (10.07 ns) as τ_{da}, we obtained $E = 0.396$ and $R = 30.0$ Å. To check whether this determination was label-dependent, it was also carried out with DAB as the acceptor. In this case triexponential analysis of the decay of $C5^{DAN} \cdot I133^{DAB} \cdot T$ yielded lifetimes that are considerably different from those derived from biexponential analysis, indicating that the decay was more complex than biexponential. Taking the shortest triexponential lifetime (2.94 ns) as τ_{da}, we obtained $E = 0.824$ and $R = 32$ Å, in reasonable agreement with that obtained with DDP as the acceptor. We noted, however, that this short lifetime is comparable to the pulse width of the instrument's excitation source (~2 ns), so that its determination is not very reliable. Furthermore, the accuracy of distance calculation is lower with very high energy transfer efficiencies. For these reasons, only distances obtained from the DAN-DDP couple

TABLE 2 Parameters of fluorescence decay and RET between Cys^{133} of TnI and selected TnC residues in the Ca^{2+} state

Materials	τ_1	τ_2	τ_3	χ^2/N	τ_d	τ_{da}	E	R_o	R
$C41^{DAN} \cdot I \cdot T$, $+Ca^{2+}$	15.15 (1.00)			1.6					
	15.11 (1.00)	82.20 (.000)		1.5					
$C41^{DAN} \cdot I \cdot T$, $-Ca^{2+}$	14.76 (1.00)			2.7					
	14.63 (.999)	46.74 (.001)		2.2					
$C41^{DAN} \cdot I^{DAB} \cdot T$, $+Ca^{2+}$	13.05 (1.00)			21.9					
	7.41 (.615)	16.99 (.385)		1.8	15.15	7.41	0.510	40.7	40.4
	6.08 (.504)	15.36 (.484)	26.15 (.012)	1.5					
$C41^{DAN} \cdot I^{DAB} \cdot T$, $-Ca^{2+}$	12.81 (1.00)			3.4					
	11.94 (.944)	21.19 (.056)		1.7	14.76	11.94	0.205	39.5	49.5
$C41^{DAN} \cdot I^{DDP} \cdot T$, $+Ca^{2+}$	13.34 (1.00)			6.3	15.15	13.34	0.119	27.5	38.4
	12.97 (.991)	31.36 (.009)		4.4					
$C41^{DAN} \cdot I^{DDP} \cdot T$, $-Ca^{2+}$	13.17 (1.00)			3.3	14.76	13.17	0.108	27.4	39.0
	12.79 (.990)	29.85 (.010)		2.0					
$C5^{DAN} \cdot I \cdot T$	16.78 (1.00)			3.6					
	16.68 (.999)	62.64 (.001)		3.6					
$C5^{DAN} \cdot I^{DAB} \cdot T$	7.20 (.595)	18.11 (.405)		2.9					
	2.94 (.426)	14.29 (.523)	24.22 (.051)	2.1	16.78	2.94	0.824	41.3	32.0
$C5^{DAN} \cdot I^{DDP} \cdot T$	10.07 (.750)	19.14 (.250)		1.2	16.78	10.07	0.396	28.0	30.0
	9.85 (.716)	18.40 (.281)	29.47 (.003)	1.2					
$C12^{DAN} \cdot I \cdot T$	18.71 (1.00)			2.5					
	18.62 (.999)	54.79 (.001)		2.2					
$C12^{DAN} \cdot I^{DDP} \cdot T$	7.83 (.563)	19.09 (.437)		2.8					
	4.34 (.290)	11.86 (.413)	20.20 (.297)	1.6	18.7	4.34	0.767	28.5	23.4

τ_1, τ_2, τ_3 are lifetimes of decay components. Fractional amplitudes are in parentheses. χ^2/N is the quality of fit parameter, defined as $(1/N)\ \Sigma_{i=1}^{N}(I_{ic} - I_{ie})^2/I_{ie})$, where I_{ic} and I_{ie} are calculated and experimental intensities for the ith channel, respectively, and N is the number of channels. τ_d and τ_{da} are donor lifetimes in the absence and presence of acceptor, respectively, used in the calculation of E, the energy transfer efficiency (Eq. 1). R_0 is the critical transfer distance (Eq. 3); R is the separation distance (Eq. 2).

TABLE 3 Summary of the measured and calculated distances, and the fitted coordinates of TnI Cys133.

Materials	Acceptor used	R (Å)			
		I^{DAN}	C^{DAN}	Ave	Calc
TnC5 · I · T, $+Ca^{2+}$	DDP	27.9	30.0	29.0	33.4
TnC12 · I · T, $+Ca^{2+}$	DDP	20.7	23.4	22.1	21.1
TnC21 · I · T, $+Ca^{2+}$	DDP	29.4	27.9	28.7	25.4
TnC41 · I · T, $+Ca^{2+}$	DAB	37.2	40.4	38.8	38.6
TnC49 · I · T, $+Ca^{2+}$	DAB	36.5	43.4	40.0	40.2
TnC89 · I · T, $+Ca^{2+}$	DDP	28.8	29.3	29.1	30.6
TnC98 · I · T, $+Ca^{2+}$	DDP	29.3	28.6	29.0	30.5
TnC133 · I · T, $+Ca^{2+}$	DAB	40.6	45.1	42.9	41.4
TnC158 · I · T, $+Ca^{2+}$	DAB	38.2	39.2	38.9	36.3
		(X = 45.7, Y = 29.1, Z = 3.7, r^2/N = 5.0)			
TnC5 · I · T, $-Ca^{2+}$	DDP	36.4	33.9	35.2	39.7
TnC12 · I · T, $-Ca^{2+}$	DDP	30.7	31.1	30.9	27.8
TnC21 · I · T, $-Ca^{2+}$	DDP	33.9	33.3	33.6	33.1
TnC41 · I · T, $-Ca^{2+}$	DAB	43.5	49.5	46.5	42.8
TnC49 · I · T, $-Ca^{2+}$	DAB	43.6	43.4	43.5	41.9
TnC89 · I · T, $-Ca^{2+}$	DDP	35.7	31.0	33.4	41.8
TnC98 · I · T, $-Ca^{2+}$	DDP	43.7	37.3	40.5	41.2
TnC133 · I · T, $-Ca^{2+}$	DAB	48.6	51.7	50.2	47.9
TnC158 · I · T, $-Ca^{2+}$	DAB	48.1	47.9	48.0	44.7
		(X = 55.4, Y = 32.9, Z = 10.8, r^2/N = 15.0)			
TnC5 · I, $+Ca^{2+}$	DDP	27.9		27.9	31.4
TnC12 · I, $+Ca^{2+}$	DDP	20.5	24.3	22.4	19.0
TnC41 · I, $+Ca^{2+}$	DAB	36.9	37.8	37.4	37.1
TnC49 · I, $+Ca^{2+}$	DAB	37.7	39.4	38.6	38.9
TnC98 · I, $+Ca^{2+}$	DDP	29.4	31.1	30.3	30.1
		(X = 44.4, Y = 30.7, Z = 3.6, r^2/N = 4.7)			
TnC5 · I, $-Ca^{2+}$	DDP	41.9		41.9	43.4
TnC12 · I, $-Ca^{2+}$	DDP	41.0	30.7	35.9	33.5
TnC41 · I, $-Ca^{2+}$	DAB	49.4	51.9	50.7	52.8
TnC49 · I, $-Ca^{2+}$	DAB	46.6	57.2	51.9	50.4
TnC98 · I, $-Ca^{2+}$	DDP	49.1	41.3	45.2	45.6
		(X = 54.9, Y = 33.4, Z = 25.6, r^2/N = 2.9)			

Each distance was measured with the DAN donor on TnI (I^{DAN}) or on TnC (C^{DAN}). X, Y, Z (in Å) are the fitted coordinates of TnI Cys[133] in reference to the coordinate system of the $2Ca^{2+}$ · TnC crystal structure (27). r^2/N is defined in Eq. 5. Calc are the calculated distances. Other conditions are the same as for Fig. 2.

were used in the distance geometry calculations for this group of complexes. Again, because the data for other members of this group had similar characteristics (with the exception of C12; see below), they were treated in the same manner; the resultant distances are presented in Table 3.

For the C12 · I133 · T complex, the donor decay in the presence of acceptor has a component of very short lifetime in the triexponential results, even when DDP was used as the acceptor (Table 2), as in the case above, in which DAB was used for the second group of complexes. This leads to the conclusion that the distance between residue 12 of TnC and Cys[133] of TnI in the ternary complex is likely to be considerably shorter than the R_o of the DAN-DDP couple (~30 Å). Using the shortest lifetime from the triexponential analysis as τ_{da}, we obtained R = 23.4 Å, recognizing, however, that it can only be taken as an upper limit. This point will be taken up in more detail in the distance geometry calculations below.

Distance geometry calculations

For the Ca^{2+} state, the α-carbon coordinates of TnC residues were taken from the structure of $4Ca^{2+}$ · TnC obtained by molecular modeling (Herzberg et al., 1986). We took as measured distances the averages of the two measurements with interchanged donor-acceptor locations (Table 3). We found that the coordinates (in Å, origin and axes shown in Fig. 2) of TnI Cys[133] that minimized r^2/N are (X, Y, Z) = (45.7, 29.1, 3.7), with r^2/N = 5.0 (Table 3). As noted earlier, the measured distance between TnC Cys[12] and TnI Cys[133] of 22.1 Å is only an upper bound. To examine the effect of this on the analysis, we repeated the fitting procedure, varying this distance from 24 to 16 Å. The resulting coordinates for TnI Cys[133] were only minimally affected. The lowest r^2/N (4.8) was obtained by taking 20 Å as the measured distance, which yielded (X, Y, Z) = (45.6, 30.1, 4.4), very similar to those obtained using 22.1 Å. The fitting was also carried out with this distance omitted, which yielded (X, Y, Z) = (45.6, 30.0, 4.3,) and r^2/N = 6.1, nearly identical to the coordinates above. Thus the same position for TnI Cys[133] was obtained without using the TnC Cys[12] to TnI Cys[133] distance at all. We conclude that 20 Å is the best estimate for this distance, and that the position of TnI Cys[133] is not very sensitive to the value of this distance. In fact, omitting any one of the distances in the set did not change the fitted position of TnI Cys[133] significantly. These results indicate that the chosen nine distances are suitable and sufficient for determining the position of TnI Cys[133] relative to TnC, and highlight the robustness of our analysis procedure, as well as the reliability of our distance measurements.

To estimate the uncertainties associated with the X, Y, Z values determined above, we used the following semiquantitative method: a Gaussian distribution was assumed for the errors associated with the distance measurements. Because there are nine distances and only two measurements for each, the standard deviation for the Gaussian distribution was taken as the root mean square of nine values, each a difference between either one of the measured distances and their mean (Table 3). This was calculated to be 1.6 Å. A Monte Carlo procedure was then used to add random errors within the Gaussian envelope to each distance. The set of distances so generated was then used to determine X, Y, Z as described above. This was repeated 200 times, after which the values were averaged and the standard deviations calculated. The results were (X, Y, Z) = (45.4 ± 1.3, 29.4 ± 2.8, 4.2 ± 2.9). Carrying out this procedure 400 times produced no significant difference in the results. Although not rigorous, this method allows us to estimate that the averaged uncertainty in X, Y, Z is ~2.4 Å.

The same analysis was applied to the distances measured in the Ca^{2+}-free state (i.e., EGTA + Mg^{2+}) (Table 3), using TnC coordinates derived from the crystal structure of $2Ca^{2+}$ · TnC (Herzberg and James, 1988), in which the high-affinity sites were occupied by Ca^{2+}, and the low-affinity activation sites were unoccupied. The fitted coordi-

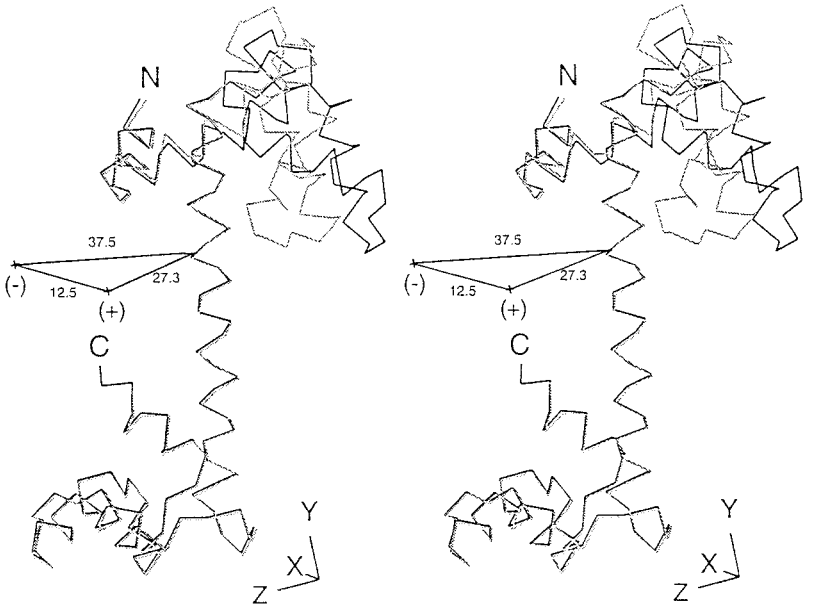

FIGURE 2 Stereo view of superimposed crystallographic structures (backbone a-carbons) of $2Ca^{2+} \cdot$ TnC (*gray*) and hypothetical $4Ca^{2+} \cdot$ TnC (*dark*) with their C-terminal lobes and central helices aligned. The major difference is in the position of helices B and C, which are close to the central helix in the $2Ca^{2+} \cdot$ TnC structure (representing the Ca^{2+}-free state) and away from the central helix in the $4Ca^{2+} \cdot$ TnC structure (representing the Ca^{2+} state). The locations of TnI Cys^{133} in the ternary Tn complex determined in this work are shown for both the Ca^{2+} and Ca^{2+}-free states (+ and −, respectively). The numbers indicate the distances (in Å) measured from the α-carbon of TnC Met^{83} and between the two positions of TnI Cys^{133} in the two metal states.

nates are (X, Y, Z) = (55.4, 32.9, 10.8), with an averaged uncertainty of, again, ~2.4 Å, determined by the same procedure as the above. This result shows that TnI Cys^{133} moves by 12.5 Å from its position in the Ca^{2+} state and is further from TnC.

The distances between TnI Cys^{133} and TnC Cys^{5}, Cys^{12}, Cys^{41}, Cys^{49}, and Cys^{98} were also measured in the binary TnC · TnI complexes, and were subjected to the same least-squares distance geometry analysis (Table 3). In the Ca^{2+} state, the measured distances were almost identical to their counterparts in the ternary complexes, giving rise to nearly the same position for TnI Cys^{133} (Table 3); in the Ca^{2+}-free state, Cys^{133} moves away from TnC to a position that is also similar to that for the ternary complex. Thus TnT appears to have little effect on the conformation of this segment of TnI relative to TnC.

DISCUSSION

In our distance calculations we have assumed that the orientation factor κ^2 takes on the isotropically averaged value of 2/3. Although the validity of this assumption had been discussed in depth by others (e.g., dos Remedios and Moens, 1995; Haas et al., 1975; Perkins et al., 1984; Stryer, 1978), we would like to emphasize several points that are specific to our system. The limiting anisotropy, A_o, was measured to be 0.22 for DAN attached at Cys^{133} of TnI (Tao et al., 1990), and 0.18 (Tao et al., 1989) and 0.21 (this work) for DAN attached at TnC residues 98 and 89, respectively. These values are all considerably lower than the theoretical limit of 0.4, indicating that the donor attached at these residues is substantially depolarized by either rapid segmental motion or electronic mechanisms. The mutation sites in all of the TnC mutants were chosen to be at residues that are exposed on the surface of the TnC molecule according to the crystal structure, such that the probes attached at these sites are likely to have similar A_o values. Considerable averaging of κ^2 can therefore be expected, so that using 2/3 as its value is likely to be justified. In principle, if A_o values could be obtained for both the donor and the acceptor, the range of κ^2 values and of the distances can be calculated (Dale and Eisinger, 1974). In our case this cannot be done, because for experimental considerations, we chose to use nonfluorescent acceptors. It was suggested by Stryer (1978), however, that confidence in the assumption of $\kappa^2 = 2/3$ can be enhanced if certain experimental criteria were met. These include invariance of the measured distances with different donor-acceptor pairs and with locations of the donor-acceptor pair. Accordingly, we measured some of the distances with both DDP and DAB; although one or the other was deemed to yield more reliable results, similar distances were obtained for either acceptor (Table 2). All of the distance measurements were made with the donor on TnC, the acceptor on TnI, and vice versa. Again, essentially similar distances were obtained (Table 3). Thus our use of $\kappa^2 = 2/3$ appears to be empirically justified. In the final analysis, the fact that all of the measured distances can be incorporated into the distance geometry analysis and yielded meaningful results indicates that our measured distances are reliable in all aspects, including the choice of the value of κ^2.

For our distance geometry calculations, we have used the coordinates derived from the crystal structure of free TnC and assumed that it is unchanged in the binary TnC · TnI and the ternary Tn complex. That the two highly helical domains should retain their folding is clearly reasonable, especially because the equivalent domains in calmodulin have been shown not to change their conformations when it binds one of its targets (Ikura et al., 1992; Meador et al., 1992). Furthermore, neutron scattering studies (Olah and Trewhella, 1994) and our preliminary RET studies showed

that TnC maintains an extended structure in the TnC · TnI complex. Modeling studies found that taking the crystal structure of TnC as the conformation that it adopts in the TnC · TnI complex fitted the neutron scattering data best (Olah and Trewhella, 1994). Based on these considerations, we believe that our assumption is a reasonable one.

Nevertheless, we attempted to address the question of whether the two TnC domains maintain their relative dispositions in the ternary Tn complex as follows: first, we carried out the minimization procedure, using, separately, the five distances to N-terminal domain residues (5, 12, 21, 41, 49) and the four distances to C-terminal domain residues (89, 98, 133, 158). The results for the $+Ca^{2+}$ state were (X, Y, Z) = (35.5, 25.1, 11.2), r^2/N = 1.9, and (44.6, 24.5, −3.8), r^2/N = 0.1, derived from the N- and C-terminal distances, respectively. Assuming that the discrepancy between the two positions is due to a difference in the relative orientations of the two TnC domains, we used the program Midas (UC San Francisco) to alter this orientation by rotations about the N-Cα and Cα-C bonds at various residues along the central helix. We found that the rotations of ϕ = 16.3° and ψ = 44.1° at residue 78 could make the two positions nearly coincident; rotations at other residues failed to bring this about. Because residue 78 is almost at the N-terminus of the central helix, this operation resulted in a small tilt of the N-terminal domain while the molecule remained essentially extended. Whereas this analysis shows that the conformation of TnC in the Tn complex may differ slightly from that of the crystal structure, we stress that, for several reasons, this is in no way a definitive analysis. First, the fact that the two positions are different from each other may simply be due to errors in the determinations, particularly because fewer distances are used in each set. Second, we clearly have not searched for all possible relative orientations of the two domains; for example, we have not attempted to carry out the rotations at more than one residue on the central helix at the same time. Third, we do not have enough distance constraints to determine both the location of TnI Cys^{133} and the relative orientations of the two TnC domains. In works that have already been initiated, we address this question more definitively by measuring more distances between TnC and TnI and between the two domains of TnC.

From our distance measurements it is clear that TnI Cys^{133} is very close to residue 12 of TnC. Our previous photo-cross-linking results showed that a photoreactive probe attached at residue 12 of TnC cross-links primarily to the segment of TnI at or near Met^{134} (Kobayashi et al., 1994). Thus the cross-linking and the RET results are in good agreement here, which is not always the case in other situations (Chantler et al., 1991).

Among our measured distances, that between Cys^{133} of TnI and Cys^{98} of TnC was measured previously with DAB only as the acceptor, and was reported to range from 27 Å to 42 Å in the Ca^{2+} state (Tao et al., 1989). All of the decay parameters were reproduced in the present work, but based on the results obtained here with DDP as the acceptor, we conclude that 29 Å is a better determination of this distance. This finding underscores the importance of using donor-acceptor pairs with the appropriate R_o value in RET distance measurements. Note that an increase in this distance in the Ca^{2+}-free state is also reproduced here.

The fitted positions of TnI Cys^{133} in the TnC coordinate system are illustrated in Fig. 2. The $2Ca^{2+}$ · TnC and the $4Ca^{2+}$ · TnC structures, which differ mainly at the B and C helices, are superimposed so that the locations of TnI Cys^{133} in the two metal binding states can be displayed simultaneously. In the presence of Ca^{2+}, TnI Cys^{133} is located below helix A, 27.2 Å laterally from the α-carbon of Met^{83} of helix D. It is clearly closer to the N- than to the C-terminal domain, providing further support for the antiparallel arrangement of TnI and TnC (Farah et al., 1994). It is also clearly below and not on top of the N-terminal domain. In the model for the structure of $4Ca^{2+}$ · TnC · TnI (Olah and Trewhella, 1994), TnI is depicted with its first and last 50 residues forming so-called cap regions below and above the C- and N-terminal domains of TnC, respectively (here the antiparallel arrangement is assumed). The caps are linked by a 79-residue α-helix that makes one turn around the central helix of TnC. This model would place TnI Cys^{133} just above the N-terminal domain of TnC. Our results obtained in both the binary and the ternary complexes are clearly not compatible with this. It seems that although the overall features of this model might be correct, the exact folding of TnI in the TnC · TnI complex appears to be more complex than that proposed.

In the Ca^{2+}-free state, TnI Cys^{133} moved further away from TnC Met^{83} by 10.3 Å, and slightly upward toward, but remaining underneath, the N-terminal lobe of TnC. Because TnI Cys^{133} has been shown to move toward actin in reconstituted thin filaments under this condition (Tao et al., 1990), it may be presumed that the movement observed here is also in the direction of actin. In this respect it is interesting to note that the location of TnI Cys^{133} is on the side of the central helix of TnC roughly opposite the B-C helices. It was proposed that the binding of Ca^{2+} to the activation sites of TnC causes the movement of the B-C helices, thereby exposing a hydrophobic patch with which some as yet unidentified TnI segment can interact (Herzberg et al., 1986). Further events in the regulatory process have not been defined, but the simplest hypothesis is that the segment of TnI that is attached to TnC via the hydrophobic patch in the presence of Ca^{2+} moves to actin in the absence of Ca^{2+} when the patch is not open. Our findings here would make this difficult to envision and argue against this simple hypothesis. Instead, they suggest a scenario in which the Ca^{2+}-dependent interaction between the TnI segment and the hydrophobic patch in TnC induces conformational changes in the complex that modulate the affinity of the Cys^{133} region of TnI for actin vis-à-vis that for TnC. Clearly, further work will be needed to clarify this point.

In conclusion, we have shown that when stringent experimental regimes are used, RET-determined distances can be

used to locate a certain residue in complexes such as Tn. This approach clearly cannot compete with x-ray crystallography or multinuclear NMR structural determinations in terms of resolution or wealth of information, but for systems that are resistant to high-resolution technques, it may provide important structural and functional information. Work is under way in our laboratory to locate other important residues in the Tn complex.

We thank Dr. Zenon Grabarek for critically reviewing the manuscript and Dr. Knut Langsetmo for help with computer modeling.

This work was supported by grants from the National Institutes of Health (AR21673 to TT and HL 5949 to JG).

REFERENCES

Botts, J., J. F. Thomason, and M. F. Morales. 1989. On the origin and transmission of force in actomyosin subfragment 1. *Proc. Natl. Acad. Sci. USA.* 86:2204–2208.

Chantler, P. D., T. Tao, and W. F. Stafford. 1991. On the relationship between distance information derived from cross-linking and from resonance energy transfer, with specific reference to sites located on myosin heads. *Biophys. J.* 59:1242–1250.

Dalbey, R. E., J. Weiel, and R. G. Yount. 1983. Forster energy transfer measurements of thiol 1 to thiol 2 distances in myosin subfragment 1. *Biochemistry.* 22:4696–4706.

Dale, R. E., and J. Eisinger. 1974. Intramolecular distances determined by energy transfer. Dependence on orientational freedom of donor and acceptor. *Biopolymers.* 13:1573–1605.

Dong, W.-J., M. Chandra, J. Xing, M. She, R. J. Solaro, and H. C. Cheung. 1997. Phosphorylation-induced distance change in a cardiac muscle troponin I mutant. *Biochemistry.* 36:6754–6761.

dos Remedios, C. G., and P. D. J. Moens. 1995. Fluorescence resonance energy transfer spectroscopy is a reliable "ruler" for measuring structural changes in proteins. *J. Struct. Biol.* 115:175–185.

Fairclough, R. H., and C. R. Cantor. 1978. The use of singlet-singlet transfer to study macromolecular assemblies. *Methods Enzymol.* 28: 347–379.

Farah, C. S., C. A. Miyamoto, C. H. I. Ramos, A. C. R. da Silva, R. B. Quaggio, K. Fujimori, L. B. Smillie, and F. C. Reinach. 1994. Structural and regulatory functions of the NH_2- and COOH-terminal regions of skeletal muscle troponin I. *J. Biol. Chem.* 269:5230–5240.

Farah, C. S., and F. C. Reinach. 1995. The troponin complex and regulation of muscle contraction. *FASEB J.* 9:755–767.

Fujimori, K., M. Sorenson, O. Herzberg, J. Moult, and F. C. Reinach. 1990. Probing the calcium-induced conformational transition of troponin-C with site-directed mutants. *Nature.* 345:182–184.

Gong, B.-J., Z. Wang, T. Tao, and J. Gergely. 1994. Troponin-C remains extended in the ternary troponin complex. *Biophys. J.* 66:A346.

Grabarek, Z., R.-Y. Tan, J. Wang, T. Tao, and J. Gergely. 1990. Inhibition of mutant troponin C activity by an intra-domain disulphide bond. *Nature.* 345:132–135.

Grabarek, Z., T. Tao, and J. Gergely. 1992. Molecular mechanism of troponin-C function. *J. Muscle Res. Cell Motil.* 13:383–393.

Greaser, M. L., and J. Gergely. 1973. Purification and properties of the components from troponin. *J. Biol. Chem.* 248:2125–2133.

Haas, E., M. Wilchek, E. Katchalsky-Katzir, and I. Z. Steinberg. 1975. Distribution of end-to-end distances of oligopeptides in solution as estimated by energy transfer. *Proc. Natl. Acad. Sci. USA.* 72:1807–1811.

Herzberg, O., and M. N. G. James. 1985. Structure of the calcium regulatory muscle protein troponin-C at 2.8 Å resolution. *Nature.* 313: 653–659.

Herzberg, O., and M. N. G. James. 1988. Refined crystal structure of troponin C from skeletal muscle at 2.0 Å resolution. *J. Mol. Biol.* 203:761–779.

Herzberg, O., J. Moult, and M. N. G. James. 1986. A model for the Ca^{2+}-induced conformational transition of troponin C. *J. Biol. Chem.* 261:2638–2644.

Ikura, M., G. M. Clore, A. M. Gronenborn, G. Zhu, C. B. Klee, and A. Bax. 1992. Solution structure of a calmodulin-target peptide complex by multidimensional NMR. *Science.* 256:632–638.

Kekic, M., W. Huang, P. D. Moens, B. D. Hambly, and C. G. dos Remedios. 1996. Distance measurements near the myosin head-rod junction using fluorescence spectroscopy. *Biophys. J.* 71:40–47.

Kobayashi, T., T. Tao, J. Gergely, and J. H. Collins. 1994. Structure of the troponin complex. Implications of photocross-linking of troponin I to troponin C thiol mutants. *J. Biol. Chem.* 269:5725–5729.

Luo, Y., J.-L. Wu, J. Gergely, and T. Tao. 1997. Troponin T and Ca^{2+} dependence of the distance between Cys^{48} and Cys^{133} of troponin I in the ternary troponin complex and reconstituted thin filaments. *Biochemistry.* 36:11027–11035.

Meador, W. E., A. R. Means, and F. A. Quiocho. 1992. Target enzyme recognition by calmodulin: 2.4 Å structure of a calmodulin-peptide complex. *Science.* 257:1251–1255.

Miki, M., S. O'Donoghue, and C. dos Remedios. 1992. Structure of actin observed by fluorescence resonance energy transfer spectroscopy. *J. Muscle Res. Cell Motil.* 13:132–145.

Olah, G. A., S. E. Rokop, C.-L. A. Wang, S. L. Blechner, and J. Twewhella. 1994. Troponin I encompasses an extended troponin C in the Ca^{2+}-bound complex: a small-angle x-ray and neutron scattering study. *Biochemistry.* 33:8233–8239.

Olah, G. A., and J. Trewhella. 1994. The structure of $4Ca^{2+}$·troponin C complexed with troponin I by small-angle scattering. *Biophys. J.* 66: A311.

Park, H.-S., T. Tao, and P. D. Chantler. 1991. Proximity relationships between sites on myosin and actin. *Biochemistry.* 30:3189–3195.

Pearlstone, J. R., B. D. Sykes, and L. B. Smillie. 1997. Interactions of structural C and regulatory N domains of troponin C with repeated sequence motifs in troponin I. *Biochemistry.* 36:7601–7606.

Perkins, W. J., J. Weiel, J. Grammer, and R. G. Yount. 1984. Introduction of a donor-acceptor pair by a single protein modification. *J. Biol. Chem.* 259:8786–8793.

Saijo, Y., S. Takeda, A. Scherer, T. Kobayashi, Y. Maeda, H. Taniguchi, M. Yao, and S. Wakatsuki. 1997. Production, crystallization, and preliminary x-ray analysis of rabbit skeletal muscle troponin complex consisting of troponin C and fragment (1–47) of troponin I. *Protein Sci.* 6:916–918.

Slupsky, C. M., and B. D. Sykes. 1995. NMR solution structure of calcium-saturated skeletal muscle troponin C. *Biochemistry.* 34: 15953–15964.

Small, E. W., and I. Isenberg. 1976. The use of moment index displacement in analyzing fluorescence time-decay data. *Biopolymers.* 15:1093–1100.

Stryer, L. 1978. Fluorescence energy transfer as a spectroscopic ruler. *Annu. Rev. Biochem.* 47:819–846.

Sundaralingam, M., R. Bergstrom, G. Strasburg, S. T. Rao, M. Greaser, and B. C. Wang. 1985. Molecular structure of troponin C from chicken skeletal muscle at 3 Å resolution. *Science.* 227:945–948.

Tao, T., and J. Cho. 1979. Fluorescence lifetime quenching studies on the accessibilities of actin sulfhydryl sites. *Biochemistry.* 18:2759–2765.

Tao, T., B.-J. Gong, and P. C. Leavis. 1990. Calcium-induced movement of troponin-I relative to actin in skeletal muscle thin filaments. *Science.* 247:1265–1372.

Tao, T., E. Gowell, G. M. Strasburg, J. Gergely, and P. C. Leavis. 1989. Ca^{2+} dependence of the distance between Cys-98 of troponin C and Cys-133 of troponin I in the ternary troponin complex. Resonance energy transfer measurements. *Biochemistry.* 28:5902–5908.

Tao, T., M. L. Lamkin, and S. S. Lehrer. 1983. Excitation energy transfer studies of the proximity between tropomyosin and actin in reconstituted skeletal muscle thin filaments. *Biochemistry.* 22:3059–3066.

Tao, T., Y. Qian, I. Boldogh, and J. Gergely. 1995. Fluorescence lifetime, acrylamide quenching and photo-crosslinking studies of the interactions

between troponin-I and troponin-T and monocysteine mutants of troponin-C. *Biophys. J.* 68:A166.

Wang, C.-K., and H. C. Cheung. 1986. Proximity relationship in the binary complex formed between troponin I and troponin C. *J. Mol. Biol.* 191:509–521.

Wang, Z., J. Gergely, and T. Tao. 1992. Characterization of the Ca^{2+}-triggered conformational transition in troponin C. *Proc. Natl. Acad. Sci. USA.* 89:11814–11817.

Wang, Z., S. Sarkar, J. Gergely, and T. Tao. 1990. Ca^{2+}-dependent interactions between the C-Helix of troponin-C and troponin-I. Photocrosslinking and fluorescence studies using a recombinant troponin-C. *J. Biol. Chem.* 265:4953–4957.